nic arc environment. Most of the classification diagrams used, are based on Rb, the element which can be very mobile, especially during metamorphism. Some varieties of the gneisses from the Lipowe Hills massif have their equivalents in the adjoining area of the Strzelin crystalline massif (SCM) (Oberc Dziedzic, 1988, 1995). Two types of the gneisses from the SCM were dated, giving the ages of 568±6 Ma (the Strzelin gneiss, Oberc-Dziedzic et al., 2001) and 504±3 Ma (the Gościęcice gneiss, Oliver et al., 1993). The geochemical composition of the Strzelin gneiss (Szczepański, 1999) is very similar to analysed gneisses from the northern part of the Lipowe Hills.

References

HARRIS N.B.W., PEARCE J.A. and TINDLE A.G., 1986. Geochemical characteristics of collision-zone magmatism. In: Coward M.P., Ries. A.C. (eds). Collision Tectonics, *Geological Society*, 19: 67-81.

OBERC-DZIEDZIC T., 1988. Serie metamorficzne Wzgórz Strzelińskich i historia ich przeobrażeń. Sesja naukowa: Budowa, rozwój i surowce skalne krystaliniku strzelińskiego (in Polish). Instytut Nauk Geologicznych Uniwersytetu Wrocławskiego, Przedsiębiorstwo Geologiczne. Wrocław.

OBERC-DZIEDZIC T., 1995. Research problems of the Wzgórza Strzelińskie metamorphic series in the light of the analysis of borehole materials (in Polish). *Acta. Univ. Wrat., 1739, Prace Geol.-Miner.*, 50: 77-105.

OBERC-DZIEDZIC T. and PIN C., 2000. The granitoids of the Lipowe Hills (Fore-Sudetic Block) and their relationships to the Strzelin granites. *Geol. Sudetica*, 33: 17-22.

OBERC-DZIEDZIC T., KLIMAS K., KRYZA R. and FANNING M., 2001. SHRIMP zircon geochronology of the Neoproterozoic Strzelin gneiss: Evidence for the Moravo-Silesian Zone affinity of the Strzelin massif, Fore-Sudetic Block, SW Poland. *Geolines*, 13: 96-97.

PEARCE J.A., HARRIS N.J. and TINDLE A.G., 1984. Trace element discrimination for the tectonic interpretation of granitic rocks. *J.Petrol.*, 25: 956-983.

SHAW D.M., CRAMER J.J., HIGGINS M.D. and TRUSCOTT M.G., 1986. Composition of the Canadian Precambrian shield and the continental crust of the earth. In: J.B. DAWSON, J. HALL, K.H. WEDEPOHL (Editors). The nature of the lower continental crust. Blackwell Sci. Publ., Oxford.

SZCZEPAŃSKI J., 1999. Geochemistry of the orthogneisses from the Strzelin crystalline massif (SW Poland, Fore-Sudetic Block). *Geolines*, 8: 68-69.

TARNEY J., 1976. Geochemistry of Archean high-grade gneisses, with implications the origin and evolution of the Precambrian crust. In: B.F. Windley (Editor), The Early History of the Earth., pp.405-417.

WERNER C.D., 1987. Saxonian granulites-igneous or lithogenous. A contribution to the geochemical diagnosis of the original rocks in high-metamorphic complexes. In: H. GERSTENBERGER (Editor), Contributions to the geology of the Saxsonian granulite massif. *Zfl-Mitteilungen.*, 133: 221-250.

WHITE B.H and CHAPPELL A.J.R. 1974. Two contrasting granite types. *Pacific Geol.*, 8: 173-174.

WÓJCIK L., 1968. Szczegółowa mapa geologiczna Sudetów. Arkusz Ciepłowody 1:25,000. Inst. Geol. Warszawa.

Visualization of Paleostress Analysis

Rostislav MELICHAR

Department of Geology and Paleontology, Masaryk University, Kotlářská 2, 611 37 Brno, Czech Republic

In connection with work on paleostress analysis of the Ro•ná mineral deposit a new requirement for visualization of some result appears. Modern computers extend our possibility to present stress data in graphical form, so two new computer programs could be developed (Orient, WinOr) and direct and inverse tasks could be visualized.

If some stress tensor is known (e. g. $ó_1$=200 MPa in 230/30; $ó_2$=100 MPa in 123/26 and $ó_3$=10 Mpa in 0/48, see Fig. 1a), it is easy to compute value of total, normal and shear stresses on any oriented plane (see Fig. 1b, 1c and 1d). Using value of internal friction and shear strength (e. g. φ=30°, τ0=15 MPa), we are able to evaluate differences between shear stress and critical shear stress for any plane (Fig. 1e). The zero line (wide black line in white zone) divides considered equal area plot into two parts with either positive (inside) or negative (outside) deviation. The first one is a field with reactivated planes and the second one defines a field of stability. Very illustrative is equal area projection of pitch angle. Distributional function of this angle between a strike line of a fault plane and resulted slip vector has two extreme – 0° and 90°. The first one (zone of strike-slips, black zone in Fig. 1f) divides a plot into fields of normal and inverse faults and the second one (zone of dip-slips, white zone in Fig. 1f) into fields of sinistral and dextral faults.

Much more interesting is graphical presentation of paleostress inverse problems. In this case, we know fault plane, slip vector and sense of movement (e.g. plane 45/45, striae 45/45, thrust; see Fig. 2a). Based on some complicated mathematic analysis, it was possible to derive special equation for normalized shear stress $\tau' = \tau/\tau max$ in dependace on Lode parameter $m = (2ó_2 - ó_1 - ó_3)/(ó_1 - ó_3)$ and direction of main normal stresses in fault coordinate system lmn (l – parallel to striae, n – perpendicular to fault plane). In equal area projection we can plot distribution for τ' for any direction of $ó_1$, $ó_2$ and $ó_3$. The considered function gives two solutions for any s1-direction (for m = 0.5 see Fig. 2b and 2c) and similarly two solutions for any s3-direction (for m=0.5 see Fig. 2e and 2f). Very attractive is equal area plot with distribution of τ' in relationship to s2-direction. Derived function leads to one solution (for m = 0.5 see Fig.

2d), but the function has one point of singularity. This point is equivalent to m-direction (which is perpendicular to M-plane) and is very important for estimation whether some inverse solution is possible or not. Geologists usually prefer s1 and s3 in their speculations, but if we understand stress problems in graphical form, s2-direction may have key-position in our thinking.

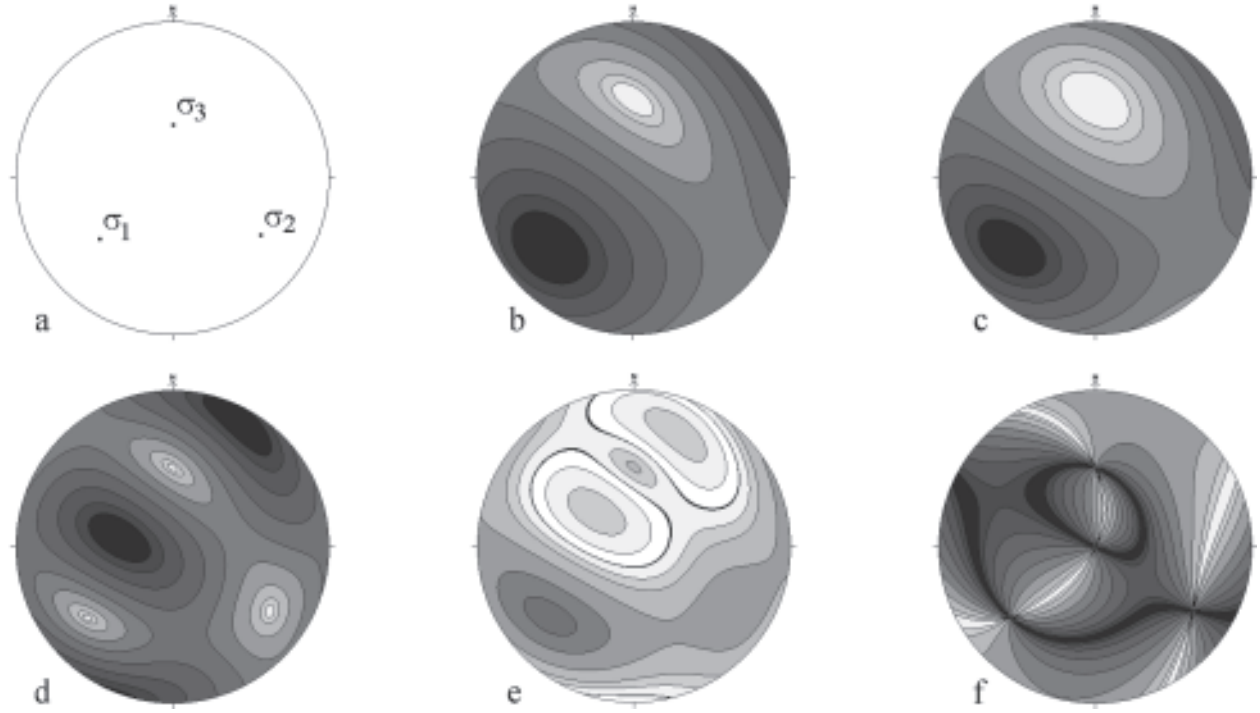

Fig. 1. Equal area projection with distribution of total stress (b), normal stress (c), shear stress (d), critical shear stress (e) and angle between slip vector and strike line (f) for one orientation of stress tensor (a). See text for explanation.

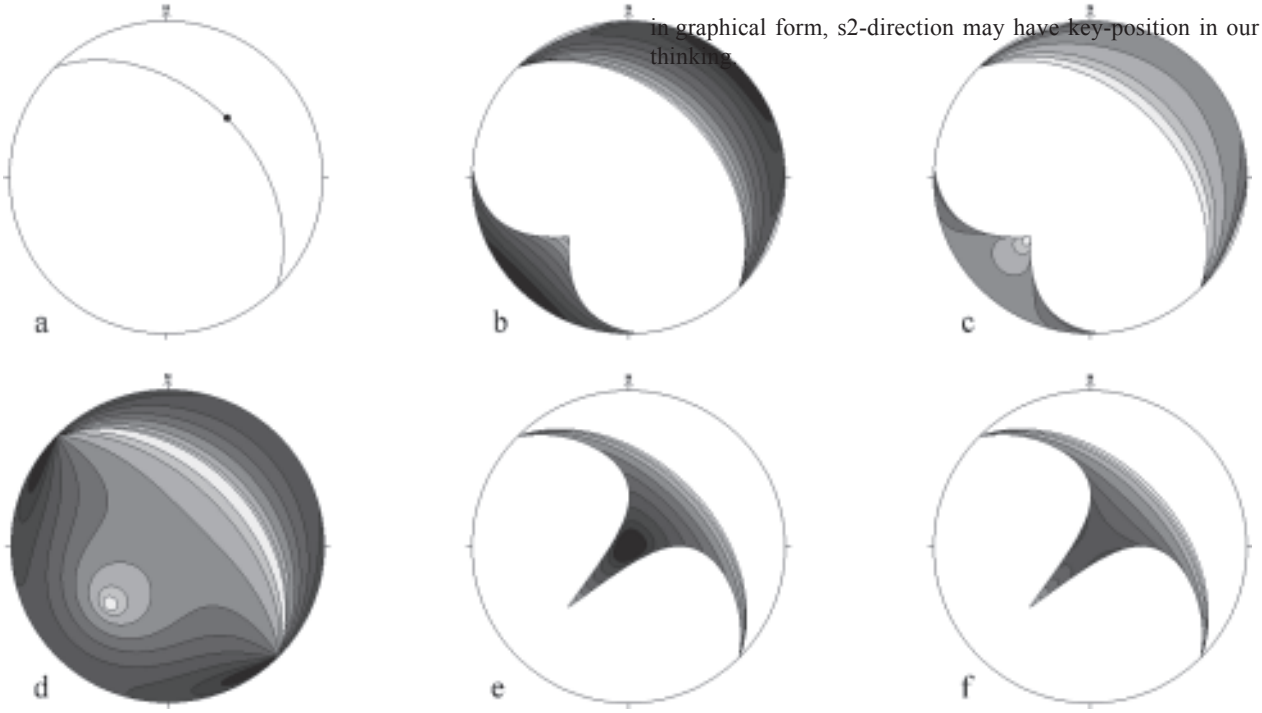

Fig. 2. Equal area plots with distribution of normalized shear stress $\tau' = \tau/\tau max$ on one fault plane (a) for diferrent directions of s1 (b, c), s2 (d) and s3 (e, f). See text for explanation.